

The effect of molecular polarity on nem/catic phase stability in 12-vertex carboranes

Jacek Pecyna^a, Richard P. Denicola^a, Harrison M. Gray^a, Bryan Ringstrand^a and Piotr Kaszynski^{a,b*}

^aDepartment of Chemistry, Organic Materials Research Group, Vanderbilt University, Nashville, TN 37235, USA; ^bFaculty of Chemistry, University of Łódź, 91403, Łódź, Poland

(Received 13 February 2014; accepted 31 March 2014)

Weakly polar–polar isosteric pairs of 12-vertex *p*-carborane [*closo*-1,12-C₂B₁₀H₁₂] (**1[12]**) and monocarbaborate [*closo*-1-CB₁₁H₁₂][−] (**2[12]**) nematic liquid crystals, in which the difference in the calculated molecular dipole moment is 11.3 D, were synthesised, and the effect of the dipole moment on nematic phase stability was investigated. The trend observed for the 12-vertex series (**1[12]**) was identical to that of the previously investigated 10-vertex series (**1[10]**) containing [*closo*-1,10-C₂B₈H₁₀] (**1[10]**) and [*closo*-1-CB₉H₁₀][−] (**2[10]**): the uniform increase in the molecular dipole moment in the pairs of mesogens does not correspond to a uniform change in the clearing temperature, *T*_{NI}. This demonstrates the role of a remote substituent in modulating the intermolecular dipole–dipole interactions. The magnitude of such interactions was calculated (using density functional theory methods) for a pair of polar (**2[12]d**–**2[12]d**) and an analogous pair of weakly polar (**1[12]d**–**1[12]d**) molecules. All results for the 12-vertex series (**1[12]**) were analysed relative to the 10-vertex analogues (**1[10]**).

Keywords: nematic; polarity; phase stability; synthesis; carboranes; DFT calculations

1. Introduction

The molecular dipole moment and its orientation with respect to the main rotational axis are important parameters considered in the design of liquid crystals for electrooptical applications.[1,2] These two parameters give rise to dielectric anisotropy, $\Delta\epsilon$, which allows for electrooptical switching of the molecules.[3,4] Despite its significance, there is little known about how the molecular dipole moment, as the *only* variable, impacts phase structure and stability. Typically, modification of the molecular dipole moment is associated with changes of the molecular geometry and dynamics, and experimental studies of the effect are hindered by lack of appropriate molecular models.

Recently, we used the concept of the isosteric polar replacement of the C–C fragment with the N⁺–B[−] fragment [5] and investigated pairs of structurally analogous and essentially geometrically identical derivatives of the [*closo*-1,10-C₂B₈H₁₀] and [*closo*-1-CB₉H₁₀][−] clusters (**1[10]** Figure 1) that display nematic behaviour.[6] The exchange of C–C for N⁺–B[−] resulted in a uniform increase of the longitudinal dipole moment ($\mu_{||}$) by about 12 D in the pairs of weakly polar (**1[10]**) and polar (**2[10]**) derivatives. Surprisingly, the uniform increase of $\mu_{||}$ did not result in a uniform change of the clearing temperature *T*_{NI} in the series. This result was rationalised by differential dielectric screening of the dipole–dipole interactions by the ester molecular subunits. It is worth mentioning that one of the compounds, ester **2[10]e**,

was found to have a record high dielectric anisotropy ($\Delta\epsilon$) of 113, [7] and for this reason, polar mesogens of structure **2** are of interest for practical applications. In order to verify the general validity of findings for the 10-vertex clusters and search for new materials with high $\Delta\epsilon$, we expanded our investigations to the 12-vertex analogues **1[12]** (Figure 1).

Here, we report a series of weakly polar (**1**)–polar (**2**) isosteric pairs of nematic 12-vertex cluster derivatives, **1[12]b**–**1[12]f**, in which the C–C fragment is replaced with the polar N⁺–B[−] fragment. We analysed the effect of the increase of the dipole moment within the 12-vertex series itself, and also considered the effect of the cluster size (12-vertex vs. 10-vertex) on phase stability.

2. Results

2.1 Synthesis

Colourless esters, **1[12]b**–**1[12]f**, were obtained from carboxylic acid **3[12]** (series **1[12]**) or **4[12]** (series **2[12]**) and the appropriate phenol or cyclohexanol (Scheme 1). Ester **1[12]a** was not prepared due to low yield of the process.[6] The preparation of acid **4[12]** expanded on our previous results obtained for diazotisation of [*closo*-1-CB₉H₈-1-COOH-6-NH₃] and [*closo*-1-CB₁₁H₁₁-12-NH₃] in 4-methoxypyridine solutions, which directly leads to the corresponding 6-pyridinium acids [*closo*-1-CB₉H₈-1-COOH-6-(4-MeOC₃H₄N)] and [*closo*-1-CB₁₁H₁₁-12-(4-MeOC₃H₄N)], respectively, through unstable diazonium intermediates.[8,9] Thus, diazotisation of amino acid

*Corresponding author. Email: piotr.kaszynski@vanderbilt.edu

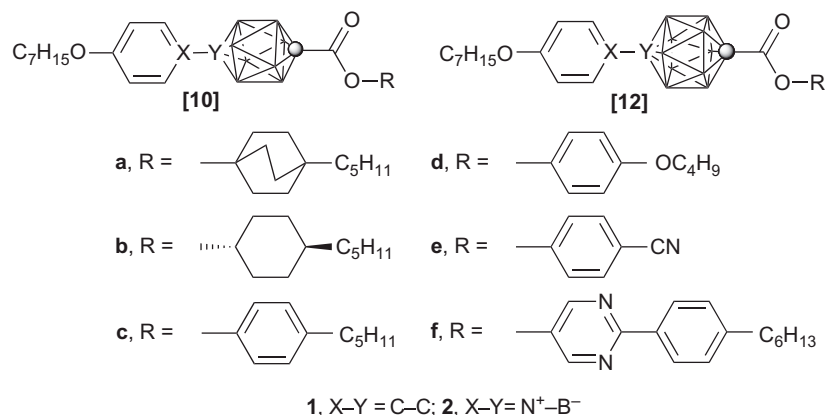
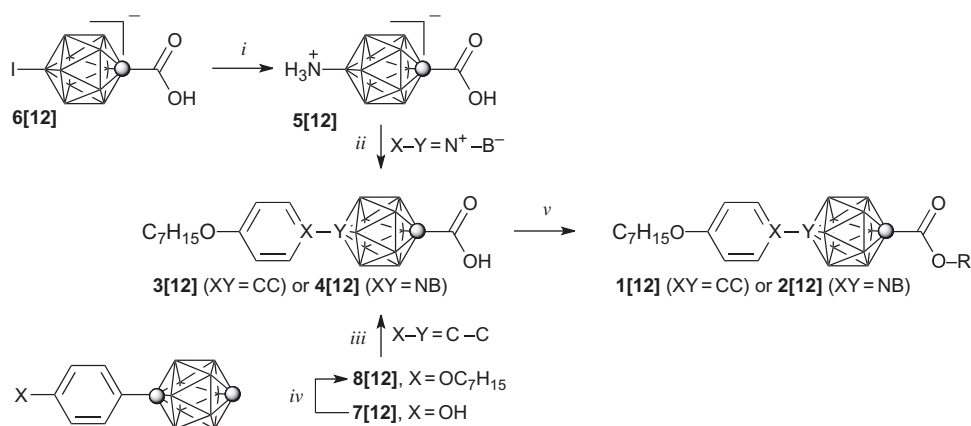


Figure 1. Structures of nematics derived from 10-vertex (**[10]**) and 12-vertex (**[12]**) clusters. Each vertex represents a BH fragment and the sphere is a carbon atom.



Scheme 1. Synthesis of esters **1[12]** and **2[12]**. Reagents and conditions: (i) Pd₂dba₃, 2-(Chx₂P)biphenyl, LiHMDS, tetrahydrofuran (THF), reflux, 72 h; (ii) 4-heptyloxyphenyl, [NO]⁺[PF₆]⁻, -15°C, 8 h; (iii) 1. *n*-BuLi, THF, -78°C; 2. CO₂; 3. H₃O⁺; (iv) C₇H₁₅OTs, K₂CO₃, [NBu₄]⁺[Br]⁻, CH₃CN, reflux, 12 h; (v) 1. (COCl)₂, 2. ROH, Pyr.

[*closo*-1-CB₁₁H₁₀-1-COOH-12-NH₃] (**5[12]**) with [NO]⁺[PF₆]⁻ in a neat solution of 4-heptyloxyphenyl gave acid **4[12]** in 6% yield. The prerequisite amino acid **5[12]** was obtained in 40% yield by Pd-catalysed amination of iodo acid [*closo*-1-CB₁₁H₁₀-1-COOH-12-I]⁻ (**6[12]**) [**10**] using conditions described for the 10-vertex analogue.^[11,12]

Acid **3[12]** [**13**] was prepared in three steps from 1-(4-hydroxyphenyl)-*p*-carborane [**14**] (**7[12]**, Scheme 1). Thus, phenol **7[12]** was O-alkylated with heptyl tosylate to facilitate separation of the resulting heptyloxyphenyl derivative **8[12]** from the alkylating reagent, giving the desired product **8[12]** in higher yield (89%) compared to direct arylation of *p*-carborane with 1-heptyloxy-4-iodobenzene.^[15] Carboxylic acid **3[12]** was obtained by direct carboxylation of **8[12]** in 92%

yield, which is more convenient than a two-step preparation through its methyl ester.^[13]

For comparison purposes esters **1[10]f** and **2[10]f** were obtained from the corresponding acids **3[10]** and **4[10]** [**6**] as described for the 12-vertex analogues.

2.2 Thermal analysis

Transition temperatures and enthalpies of the mesogens were obtained by differential scanning calorimetry (DSC). Phase structures were assigned by polarising optical microscopy and the results are shown in Table 1.

Optical and thermal analyses demonstrated that all derivatives, **[12]b–[12]f**, exhibit only a nematic phase (Table 1), which is consistent with findings for the **[10]a–[10]e** series.^[6] In general, polar nematics **2** have

Table 1. Transition temperatures and enthalpies (in parentheses) for **[12]b–[12]f** and **[10]f**.^a

	X–Y	Cr	N	I
[12]b	C–C	• 73 (29.1)	• 115 (1.3)	•
	N ⁺ –B [–]	• 158 (29.4)	• 185 (0.8)	•
[12]c	C–C	• 54 (25.6)	• 103 (1.3)	•
	N ⁺ –B [–]	• 134 (15.0) ^b	(• 133 (0.7) ^c)	•
[12]d	C–C	• 53 (30.4)	• 136 (1.6)	•
	N ⁺ –B [–]	• 142 (18.6)	• 175 (1.0)	•
[12]e	C–C	• 99 (31.9)	• 124 (0.9)	•
	N ⁺ –B [–]	• 155 (29.3) ^d	(• 151 (0.4) ^e)	•
[12]f	C–C	• 81 (36.5)	• 213 (1.4) ^e	•
	N ⁺ –B [–]	• 184 (32.9)	• 263 (1.5) ^e	•
[10]f	C–C	• 100 (29.0) ^f	• 214 (1.1) ^e	•
	N ⁺ –B [–]	• 159 (31.1) ^g	• 262 (0.4) ^e	•

Notes: ^aCr, crystal; N, nematic; I, isotropic. Temperatures obtained on heating at 5K min^{–1}.

^bCr₁ 125 (16.8) Cr₂.

^cObtained on cooling.

^dCr₁ 137 (3.0) Cr₂.

^eHeating rate 10K min^{–1}.

^fCr₁ 45 (1.8) Cr₂.

^gCr₁ 147 (8.7) Cr₂.

significantly higher transition temperatures than the weakly polar analogues **1**. Consistent with our previous findings for **[10]**,^[6] the lowest clearing temperature is observed for the pentylphenol esters **[12]c** and the highest for pyrimidinol esters **[12]f** in both series **1** and **2**. Interestingly, with the exception of **[12]f**, the enthalpy of the N–I transition is generally smaller for the polar derivatives than for the weakly polar analogues.

A comparison of the two series of 12-vertex derivatives, **1**[**12**] and **2**[**12**], shows that the difference in the clearing temperatures ΔT_{NI} , defined as $T_{\text{NI}}(\mathbf{2}) - T_{\text{NI}}(\mathbf{1})$, is not uniform for all five pairs; the largest difference in clearing temperatures, $\Delta T_{\text{NI}} = 70$, is observed for pair **[12]b** (pentylcyclohexanol esters) and the lowest, $\Delta T_{\text{NI}} = 27$, for pair **[12]e** (cyanophenol esters). A plot of ΔT_{NI} values for pairs **[12]** demonstrates the same trend as observed previously for series **[10]** (Figure 2), with the ΔT_{NI} values systematically larger for the former series than those for the 10-vertex analogues. Moreover, the data reveals a reasonable linear correlation for ΔT_{NI} in both series **[10]** and series **[12]** (Figure 3). This suggests that the remote substituent has a strong and consistent impact on intermolecular interactions and hence phase stability in both series.

The available data also permits the analysis of the effect of cluster size on nematic phase stability in the two series. Thus, a comparison of T_{NI} of polar mesogens **2**[**10**] with **2**[**12**] shows good linear correlation (Figure 4), and a similar relationship was found for the weakly polar analogues, **1**[**10**] and **1**[**12**]. In general, there is comparable nematic phase stability

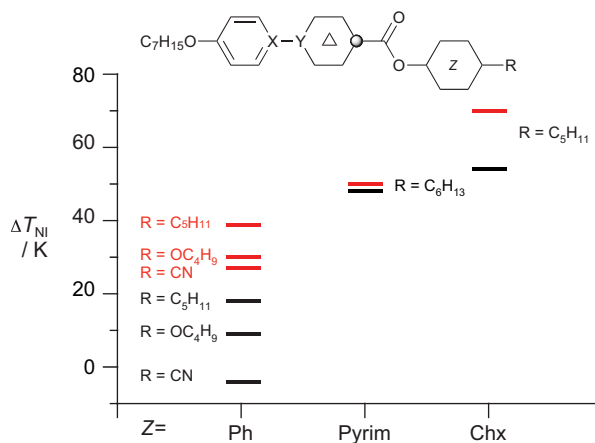


Figure 2. (colour online) A plot of the ΔT_{NI} for series **[10]** (black) and for series **[12]** (red). ΔT_{NI} represents the difference between T_{NI} of polar (**2**) and T_{NI} of weakly polar (**1**) mesogen in each series.

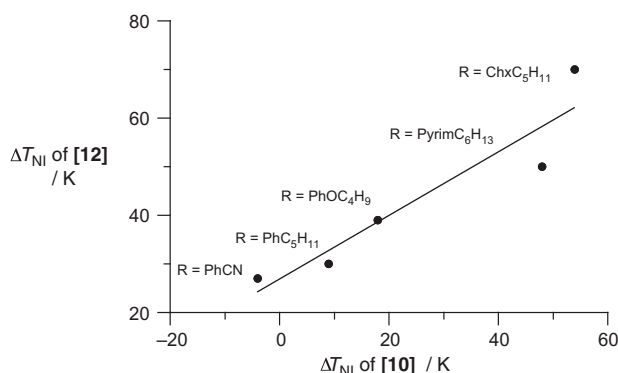


Figure 3. A plot of ΔT_{NI} for the **[12]** series versus the ΔT_{NI} of the **[10]** analogues.

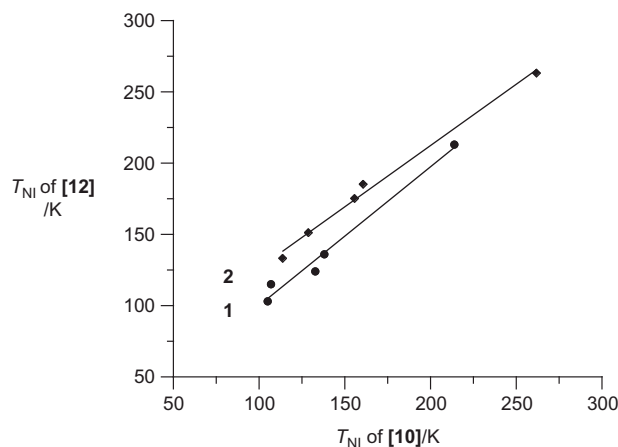


Figure 4. A plot of T_{NI} of the **[10]** series versus the T_{NI} of the **[12]** analogues for the weakly polar (circles) and polar (diamonds) derivatives. Best fit lines: $T_{\text{NI}}[\mathbf{12}] = 0.97 \times T_{\text{NI}}[\mathbf{10}] + 2.4$, $r^2 = 0.981$ for series **[1]**; $T_{\text{NI}}[\mathbf{12}] = 0.86 \times T_{\text{NI}}[\mathbf{10}] + 40.1$, $r^2 = 0.993$ for series **[2]**.

between the weakly polar analogs, **1[10]** and **1[12]**, while 12-vertex polar compounds, **2[12]**, exhibit higher mesophase stability than the 10-vertex, **1[10]**, analogs. These trends result in the observed uniformly higher ΔT_{NI} values for the 12-vertex series than for series **[10]**, as demonstrated in Figures 2 and 4.

2.3 Molecular structure and properties

For a better understanding of the impact at the molecular level of the replacement of the C–C fragment in series **1** with the N⁺–B[−] fragment in series **2**, molecular dimensions and electronic properties of the two series of nematics, **[12]b–[12]f**, were calculated in their most extended conformations at the B3LYP/6-31G(d,p) level of theory in the vacuum. Analysis of the data in Table 2 shows that replacement of C–C with N⁺–B[−] results in a significant change of the molecular dipole

Table 2. Calculated molecular parameters for **[12]b–[12]f**.^a

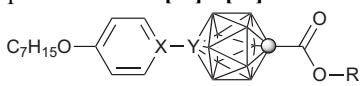
Compound	μ_{\parallel}/D	μ_{\perp}/D	μ/D	$\alpha_{\parallel}/\text{\AA}^3$	$\alpha_{\perp}/\text{\AA}^3$	$\alpha/\text{\AA}^3$	$\Delta\alpha/\text{\AA}^3$
1[12]b	1.11	1.42	1.80	89.5	47.5	42.1	61.5
2[12]b	12.16	3.02	12.53	89.6	47.7	41.9	61.7
1[12]c	1.60	1.16	1.97	94.6	46.0	48.6	62.2
2[12]c	12.77	3.13	13.14	94.6	46.2	48.4	62.3
1[12]d	0.80	1.72	1.89	94.6	44.8	49.9	61.4
2[12]d	12.07	3.42	12.54	94.4	45.0	49.5	61.4
1[12]e	7.71	0.53	7.73	88.9	39.8	49.1	56.2
2[12]e	18.99	1.88	19.08	88.7	40.0	48.6	56.2
1[12]f	3.73	1.79	4.14	121.8	52.4	69.4	75.5
2[12]f	15.38	2.38	15.56	121.5	52.6	68.9	75.5

Note: ^aObtained at the B3LYP/6-31G(d,p) level of theory.

moment and a negligible change in electronic polarisability and geometry (Table 3). Thus, the replacement increases the longitudinal component of the dipole μ_{\parallel} by 11.3 ± 0.2 D and the transverse component μ_{\perp} by an average of 1.4 D (Table 2). At the same time, electronic polarisability α_{\parallel} increases by about 0.2 \AA^3 or about 0.4%, while the average value of α slightly decreases by 0.06 \AA^3 . The polar molecules are longer by 5.2 ± 1 pm or $\sim 0.2\%$ as a result of minor expansion of the aryl–cage bond and the {*closo*-1-CB₁₁} cage by 4.5 ± 0.04 pm and 6.2 ± 0.1 pm, respectively, and contraction of the aryl ring and cage–COO bond by -3.3 ± 0.04 pm and -0.5 ± 0.04 pm, respectively (Table 3).

To shed more light on the origin of the increased nematic phase stability in polar derivatives, we assessed the interaction energy of a weakly polar pair, **1[12]d–1[12]d**, and compared it to that of its polar analogue, **2[12]d–2[12]d**. The calculations were conducted using the M06-2x functional, which reproduces non-covalent interactions reasonably well.^[16] Thus, two molecules of **1[12]d**, at equilibrium geometry, were set antiparallel at a distance of about 4 Å in vacuum and the geometry of the pair was optimised. Subsequently, the C–C fragment in **1[12]d** was replaced with the N⁺–B[−] fragment, giving two molecules of **2[12]d**, and the geometry was fully optimised again. The resulting equilibrium geometry of **2[12]d–2[12]d** is essentially the same as that of the weakly polar pair **1[12]d–1[12]d**. In the resulting molecular pairs, the {*closo*-1-CB₁₁} clusters sit above the pyridine rings with the closest B[−]⋯N intermolecular distance of about 3.6 Å. A comparison of the energies

Table 3. Selected structural parameters for **[12]b–[12]f**.^a



[12]

Compound	X–Y	$d_{C\dots X}/\text{\AA}$	$d_{X\dots Y}/\text{\AA}$	$d_{Y\dots C}/\text{\AA}$	$d_{C\dots COO}/\text{\AA}$	$L^b/\text{\AA}$
1[12]b	C–C	2.827	1.514	3.130	1.524	31.56
2[12]b	N ⁺ –B [−]	2.793	1.559	3.193	1.519	31.60
1[12]c	C–C	2.827	1.514	3.131	1.521	31.00
2[12]c	N ⁺ –B [−]	2.794	1.559	3.192	1.516	31.07
1[12]d	C–C	2.827	1.514	3.130	1.521	31.48
2[12]d	N ⁺ –B [−]	2.794	1.559	3.192	1.517	31.53
1[12]e	C–C	2.827	1.514	3.129	1.518	27.20
2[12]e	N ⁺ –B [−]	2.794	1.558	3.190	1.513	27.24
1[12]f	C–C	2.827	1.514	3.129	1.517	36.67
2[12]f	N ⁺ –B [−]	2.794	1.559	3.190	1.512	36.73
Average Δd		−0.033	0.045	0.062	−0.005	0.052
		± 0.0004	± 0.0004	± 0.001	± 0.0004	± 0.013

Notes: ^aObtained at the B3LYP/6-31G(d,p) level of theory. Distances in Å.

^bMolecular length measured as a distance between two terminal hydrogen atoms on the alkyl chains or H[⋯]N for **[12]e**.

for isolated molecules and the dimeric associates gives the interaction energy of $\Delta H = -9.7 \text{ kcal mol}^{-1}$ for **1[12]d**–**1[12]d** and $\Delta H = -22.7 \text{ kcal mol}^{-1}$ for **2[12]d**–**2[12]d** (or $\Delta G_{298} = +12.4 \text{ kcal mol}^{-1}$ and $\Delta G_{298} = +0.1 \text{ kcal mol}^{-1}$, respectively) in vacuum. Placing the molecules in a low dielectric strength medium ($\epsilon = 2.5$), typical for weakly polar mesogens, had a modest effect on the association enthalpy of **1[12]d**–**1[12]d** ($\Delta H_a = -8.2 \text{ kcal mol}^{-1}$). In contrast, the dielectric medium markedly reduced the exotherm of formation the polar pair **2[12]d**–**2[12]d** ($\Delta H_a = -15.6 \text{ kcal mol}^{-1}$). As a result, the difference in association energy between weakly polar and polar pairs, $\Delta\Delta H_a$, is $7.5 \text{ kcal mol}^{-1}$ in a dielectric medium. Thus, the calculated higher association energy for the polar derivatives corresponds to a higher melting point by nearly 90 K and higher mesophase stability by 39 K of **2[12]d** when compared to **1[12]d**.

3. Discussion and conclusions

The isoelectronic pairs of *p*-carboranes and monocarborates offer a unique opportunity to investigate the effect of the molecular dipole moment on phase stability and assist in the development of new materials for display applications. Although the preparation of pyridinium acid, **4[12]**, the key intermediate to polar mesogens **2[12]**, is low in yield at the moment, its successful synthesis permits studies of fundamental aspects of the liquid crystalline state. The preparation of amino acid **5[12]**, the precursor to **4[12]**, from $B_{10}H_{14}$, is accomplished in five steps and about 10% yield, which compares to six steps and 6% overall yield for the synthesis of 10-vertex amino acid **5[10]**.^[11] While the subsequent transformation of **5[10]** to pyridinium acid **4[10]** is done in two steps with about 50% yield,^[6] the single-step diazotisation of **5[12]** gives the desired **4[12]** in poor yield of 6%. Thus, improving the yield of the last transformation (**5[12]**→**4[12]**) would make compounds **2[12]** more attractive for further studies.

The mesogenic behaviour of compounds in series **[12]** is consistent with findings for 10-vertex series **[10]**: only nematic phases are found in both series and observed trends in T_{NI} are identical. Quantum-mechanical modelling demonstrated that

replacement of the weakly polar C–C fragment with the polar N^+B^- group in either series **[12]** or **[10]**,^[6] practically does not change either the geometry (within 0.2%) or the conformational properties of the molecules, but significantly increases the dipole moment oriented along the long molecular axis by about 11.3 and 12.0 D, respectively. Similar to the findings for the 10-vertex series **[10]**,^[6] the uniform increase of the dipole moment does not correspond to a uniform change in the clearing temperature, T_{NI} . Since the trends are the same in both series, the observed effect of the remote substituent on the ΔT_{NI} for each pair of compounds appears to be general.

The increase of molecular polarity, resulting from the C–C for N^+B^- replacement, increases the energy of intermolecular association. As calculated for two pairs of molecules, weakly polar **1[12]d**–**1[12]d** and polar **2[12]d**–**2[12]d**, this additional stabilisation by $7.5 \text{ kcal mol}^{-1}$ for the polar molecules is substantial and consistent with higher transition temperatures generally observed in series **2**. Although not calculated, it can be assumed that this association energy can be affected by remote substituents (ester residues) either through steric (molecular overlap, *c.f.* Figure 5) or electronic (dipolar interactions, dielectric screening, etc.) factors. It should be noted that the difference in the association energy was calculated without conformational search.

The change in molecular polarity also impacts the entropy of the N–I transition, ΔS_{NI} . With the exception of **[12]f**, ΔS_{NI} values calculated from the enthalpy of transition (Table 1) are about twice as large for weakly polar nematics, which suggests that polar nematics exhibit less molecular reorganisation during the N–I transition. Since both weakly polar and analogous polar nematics have essentially the same conformational space, this suggests that the polar analogues have more organised isotropic phase due to strong lateral dipole–dipole interactions. Similarly, strong dependence of ΔS_{NI} on molecular structure was previously observed for a homologous series of mesogenic dimers connected with a spacer group. In this case, lower ΔS_{NI} values were observed for the bent dimers (connectors with odd number of atoms in the chain), which was interpreted as being

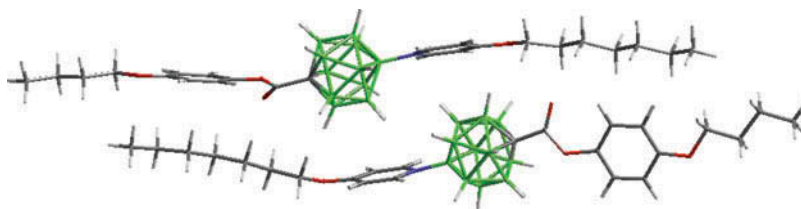


Figure 5. Optimised geometry of two molecules of **2[12]d** obtained at the M06-2x/3-21G* level of theory in vacuum.

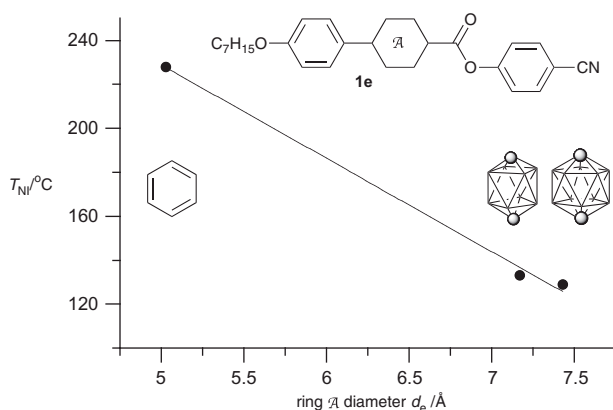


Figure 6. N–I transition temperature (T_{NI}) as a function of the diameter of ring A in **1e**.

indicative of a less-ordered nematic phase than for linear homologues (connectors with even number of atoms in the chain) having higher ΔS_{NI} values.[17]

Finally, results presented here demonstrate once again that the phase stability depends on the size of the structural elements in the rigid core.[18,19] A comparison of three isostructural mesogens **1e** shows a linear decrease of T_{NI} with increasing size of the core element A (Figure 6). Thus, **1[Ph]e**,[20] in which benzene ring has the smallest effective Van der Waals diameter d_e ,[21] possesses the highest nematic phase stability. Conversely, **1[12]e**, with the largest core element, has the lowest T_{NI} . It appears that the bulky carborane cluster near the centre of the molecule provides sufficient disruption of molecular packing arrangements and destabilises the nematic phase relative to benzene analogues. It also completely suppresses the formation of smectic phases in series **2**, which, in general, are very seldom observed in carborane-containing mesogens.[19]

Overall, the analysis of series **[12]** confirmed our previous findings for 10-vertex series **[10]**, and provided additional rare experimental data for further theoretical analysis of the fundamental issue of the role of the molecular dipole moment in mesophase stabilisation.

4. Computational details

Quantum-mechanical calculations were carried out using Gaussian 09 suite of programs.[22] Geometry optimisations for unconstrained conformers of **[12]b–[12]f** with the most extended molecular shapes were undertaken at the B3LYP/6-31G(d,p) level of theory using default convergence limits. The alkoxy group was set in an all-*trans* conformation, co-planar with the aromatic ring in the input structure. The aromatic ring and the carboxyl group were set staggered with the carborane cage, as found experimentally and computationally in related

structures. The orientation of the alkyl and carbonyloxy substituents on the alicyclic ring was set according to conformational analysis of the corresponding 1-ethyl and 1-acetoxy derivatives of cyclohexane. Optimised structures of the weakly polar compounds served as starting points for optimisation of the polar analogues after replacing the two carbon atoms with B and N.

Interaction energy in a binary system of **1[12]d** was obtained using the M06-2x functional [16] with 3-21G* basis set. Two molecules of **1[12]d** at equilibrium geometry (M06-2x/3-21G*) were aligned anti-parallel, about 4 Å apart, in the input structure, and the geometry of the pair was minimised. The resulting energy was corrected for basis set superposition error (BSSE) by running single-point calculations (M06-2x/3-21G*/M06-2x/3-21G*) at the equilibrium geometry with the keyword COUNTERPOISE = 2.[23] The optimised geometry of the weakly polar pair **1[12]d–1[12]d** served as the starting point for calculations involving the polar pair **2[12]d–2[12]d**, after replacement of the C–C fragments with the B–N. Conformational search was not attempted.

Thermodynamic parameters were requested with the FREQ keyword. The polarizable continuum model [24] was implemented using the SCRF(Solvent = Generic, Read) keyword and specified ‘epsinf = 2.25’ and ‘eps = 2.5’, and the total energies were obtained in single-point calculations with the same method.

5. Experimental

5.1 General

Reagents and solvents were obtained commercially. Reactions were carried out under Ar, and subsequent manipulations were conducted in air. NMR spectra were obtained at 128 MHz (^{11}B) and 400 MHz (^1H) in CD_3CN or CDCl_3 . ^1H NMR spectra were referenced to the solvent, and ^{11}B NMR chemical shifts were referenced to an external boric acid sample in CH_3OH that was set to 18.1 ppm. Optical microscopy and phase identification were performed using a polarised microscope equipped with a hot stage. Thermal analysis was obtained using a TA Instruments DSC using small samples of about 0.5–1.0 mg. Transition temperatures (onset) and enthalpies were obtained on heating using small samples (0.5–1 mg) and a heating rate of 5 K min^{-1} and 10 K min^{-1} under a flow of nitrogen gas, unless specified otherwise.

5.2 General procedure for preparation of esters **[12]b–[12]f**

Method A. A mixture of carboxylic acid (0.25 mmol) and anhydrous CH_2Cl_2 (1 mL) was treated with $(\text{COCl})_2$ (0.75 mmol) and a drop of dry

dimethylformamide at room temperature (RT). The mixture began to bubble, and the reaction became homogeneous within a few minutes. After 30 min, the light yellow solution was evaporated to dryness, redissolved in anhydrous CH_2Cl_2 (1.5 mL), and phenol (0.30 mmol) and a freshly distilled NEt_3 (52 μL , 0.37 mmol) were added. The reaction was stirred overnight at RT, evaporated to dryness, passed through a short silica gel plug (CH_2Cl_2), filtered through a cotton plug, and recrystallised.

Method B. The acid chloride derived from carboxylic acid (0.25 mmol) was generated as in Method A. The crude acid chloride, excess *trans*-4-pentylcyclohexanol [25] (~1 mmol), and dry pyridine (0.1 mL) were added as solvent. The mixture was heated for 3 days at 90°C, protected from moisture. At times, the reaction was cooled to RT, and minimal amounts of anhydrous CH_2Cl_2 were added to wash the sides of the flask. The product was purified as described in Method A.

5.2.1 Ester of 12-(4-heptyloxyphenyl)-*p*-carborane-1-carboxylic acid and 4-*trans*-pentylcyclohexanol (1[12]b)

It was obtained using Method B in 36% yield after chromatography (CH_2Cl_2). The ester was purified by recrystallisation from $\text{EtOAc}/\text{CH}_3\text{CN}$ (3 \times) at -40°C and then pentane (3 \times) at -20°C to give a white crystalline solid: ^1H NMR (400 MHz, CDCl_3) δ 0.88 (t, J = 7.0 Hz, 3H), 0.89 (t, J = 7.0 Hz, 3H), 0.91–1.02 (m, 2H), 1.12–1.45 (m, 18H), 1.69–1.81 (m, 5H), 1.5–3.5 (br m, 10H), 1.82–1.90 (m, 2H), 3.88 (t, J = 6.5 Hz, 2H), 4.47–4.57 (m, 1H), 6.66 (d, J = 9.0 Hz, 2H), 7.07 (d, J = 8.9 Hz, 2H); $\{^1\text{H}\}^{11}\text{B}$ NMR (128 MHz, CDCl_3) δ -13.2 (5B), -12.5 (5B). Anal. Calcd. for $\text{C}_{27}\text{H}_{50}\text{B}_{10}\text{O}_3$: C, 61.10; H, 9.49. Found: C, 61.30; H, 9.31.

5.2.2 Ester of 12-(4-heptyloxyphenyl)-*p*-carborane-1-carboxylic acid and 4-pentylphenol (1[12]c)

It was obtained using Method A in 78% yield after chromatography (CH_2Cl_2). The ester was purified by recrystallisation from $\text{EtOAc}/\text{CH}_3\text{CN}$ (3 \times) at -40°C and then pentane (3 \times) at -20°C to give a white crystalline solid: ^1H NMR (400 MHz, CDCl_3) δ 0.88 (t, J = 7.1 Hz, 3H), 0.89 (t, J = 7.0 Hz, 3H), 1.20–1.45 (m, 10H), 1.45–1.62 (m, 4H), 1.74 (quint, J = 7.1 Hz, 2H), 1.5–3.5 (br m, 10H), 2.58 (t, J = 7.7 Hz, 2H), 3.89 (t, J = 6.6 Hz, 2H), 6.68 (d, J = 9.0 Hz, 2H), 6.89 (d, J = 8.5 Hz, 2H), 7.10 (d, J = 8.9 Hz, 2H), 7.14 (d, J = 8.5 Hz, 2H); $\{^1\text{H}\}^{11}\text{B}$ NMR (128 MHz, CDCl_3) δ -13.2 (5B), -12.2 (5B).

Anal. Calcd. for $\text{C}_{27}\text{H}_{44}\text{B}_{10}\text{O}_3$: C, 61.80; H, 8.45. Found: C, 61.84; H, 8.30.

5.2.3 Ester of 12-(4-heptyloxyphenyl)-*p*-carborane-1-carboxylic acid and 4-butoxyphenol (1[12]d)

It was obtained using Method A in 62% yield after chromatography (CH_2Cl_2). The ester was purified by recrystallisation $\text{EtOAc}/\text{CH}_3\text{CN}$ (3 \times) at -40°C and then pentane (3 \times) at -20°C to give a white crystalline solid: ^1H NMR (400 MHz, CDCl_3) δ 0.88 (t, J = 6.9 Hz, 3H), 0.96 (t, J = 7.4 Hz, 3H), 1.30–1.55 (m, 10H), 1.57–1.77 (m, 4H), 1.5–3.5 (br m, 10H), 3.87 (t, J = 6.5 Hz, 2H), 3.91 (t, J = 6.5 Hz, 2H), 6.67 (d, J = 8.9 Hz, 2H), 6.81 (d, J = 9.2 Hz, 2H), 6.88 (d, J = 9.2 Hz, 2H), 7.08 (d, J = 8.9 Hz, 2H); $\{^1\text{H}\}^{11}\text{B}$ NMR (128 MHz, CDCl_3) δ -13.2 (5B), -12.3 (5B). Anal. Calcd. for $\text{C}_{26}\text{H}_{42}\text{B}_{10}\text{O}_4$: C, 59.29; H, 8.04. Found: C, 59.46; H, 8.21.

5.2.4 Ester of 12-(4-heptyloxyphenyl)-*p*-carborane-1-carboxylic acid and 4-cyanophenol (1[12]e)

It was obtained using Method A in 77% yield after chromatography (CH_2Cl_2). The ester was purified by recrystallisation from CH_3OH (3 \times) at -40°C and then *iso*-octane (3 \times) at -40°C to give a white crystalline solid: ^1H NMR (400 MHz, CDCl_3) δ 0.89 (t, J = 6.7 Hz, 3H), 1.26–1.45 (m, 8H), 1.74 (quint, J = 6.4 Hz, 2H), 1.5–3.5 (br m, 10H), 3.89 (t, J = 6.6 Hz, 2H), 6.69 (d, J = 9.0 Hz, 2H), 7.08 (d, J = 9.0 Hz, 2H), 7.15 (d, J = 8.8 Hz, 2H), 7.67 (d, J = 8.8 Hz, 2H); $\{^1\text{H}\}^{11}\text{B}$ NMR (128 MHz, CDCl_3) δ -13.2 (5B), -12.2 (5B). Anal. Calcd. for $\text{C}_{23}\text{H}_{33}\text{B}_{10}\text{NO}_3$: C, 57.60; H, 6.94; N, 2.92. Found: C, 57.34; H, 6.79; N, 2.79.

5.2.5 Ester of 12-(4-heptyloxyphenyl)-*p*-carborane-1-carboxylic acid and 2-(4-hexylphenyl)-5-hydroxypyrimidine (1[12]f)

It was obtained using Method A in 72% yield after chromatography (CH_2Cl_2). The ester was purified by recrystallisation from $\text{CH}_3\text{CN}/\text{toluene}$ (3 \times) at -40°C and then *iso*-octane (3 \times) at -40°C to give a white crystalline solid: ^1H NMR (400 MHz, CDCl_3) δ 0.881 (t, J = 7.0 Hz, 3H), 0.884 (t, J = 7.0 Hz, 3H), 1.23–1.45 (m, 14H), 1.64 (quint, J = 7.5 Hz, 2H), 1.74 (quint, J = 7.0 Hz, 2H), 1.5–3.5 (br m, 10H), 2.66 (t, J = 7.7 Hz, 2H), 3.89 (t, J = 6.5 Hz, 2H), 6.69 (d, J = 9.0 Hz, 2H), 7.08 (d, J = 9.0 Hz, 2H), 7.28 (d, J = 8.2 Hz, 2H), 8.28 (d, J = 8.2 Hz, 2H), 8.52 (s, 2H); $\{^1\text{H}\}^{11}\text{B}$ NMR

(128 MHz, CDCl₃) δ -13.2 (5B), -12.1 (5B). Anal. Calcd. for C₃₂H₄₈B₁₀N₂O₃: C, 62.31; H, 7.84; N, 4.54. Found: C, 62.58; H, 7.85; N, 4.56.

5.2.6 Ester of 10-(4-heptyloxyphenyl)-*p*-carborane(10 ν)-1-carboxylic acid and 2-(hexylphenyl)-5-hydroxypyrimidine (**1[10]f**)

It was obtained using Method A in 89% yield after chromatography (CH₂Cl₂). The ester was purified by recrystallisation from CH₃CN/toluene (2 \times) and CH₃OH/EtOAc (2 \times) to give a white crystalline solid: ¹H NMR (400 MHz, CDCl₃) δ 0.88 (t, *J* = 6.9 Hz, 3H), 0.91 (t, *J* = 6.7 Hz, 3H), 1.22–1.44 (m, 12H), 1.49 (quint, *J* = 7.3 Hz, 2H), 1.5–3.4 (br m, 8H), 1.67 (quint, *J* = 8.3 Hz, 2H), 1.83 (quint, *J* = 7.0 Hz, 2H), 2.69 (t, *J* = 7.7 Hz, 2H), 4.04 (t, *J* = 6.5 Hz, 2H), 6.98 (d, *J* = 8.7 Hz, 2H), 7.32 (d, *J* = 8.2 Hz, 2H), 7.71 (d, *J* = 8.7 Hz, 2H), 8.36 (d, *J* = 8.2 Hz, 2H), 8.86 (s, 2H); {¹H}¹¹B NMR (128 MHz, CDCl₃) δ -9.7 (8B). Anal. Calcd. for C₃₂H₄₆B₈N₂O₃: C, 64.79; H, 7.82; N, 4.72. Found: C, 65.06; H, 7.90; N, 4.57.

5.2.7 Ester of [closo-1-CB₁₁H₁₀-1-COOH-12-(1-(4-C₇H₁₅O-C₅H₄N))] and 4-*trans*-pentylcyclohexanol (**2[12]b**)

It was obtained using Method A in 46% yield after chromatography (CH₂Cl₂). The ester was purified by recrystallisation from toluene/*iso*-octane (3 \times) and then CH₃OH at -20°C (3 \times) to give a white crystalline solid: ¹H NMR (400 MHz, CDCl₃) δ 0.87 (t, *J* = 7.1 Hz, 3H), 0.89 (t, *J* = 6.8 Hz, 3H), 0.92–1.02 (m, 2H), 1.10–1.40 (m, 16H), 1.4–2.8 (br m, 10H), 1.41–1.51 (m, 2H), 1.75 (br d, *J* = 12.3 Hz, 2H), 1.81–1.95 (m, 5H), 4.16 (t, *J* = 6.5 Hz, 2H), 4.53–4.61 (m, 1H), 7.00 (d, *J* = 7.4 Hz, 2H), 8.43 (d, *J* = 7.4 Hz, 2H); {¹H}¹¹B NMR (128 MHz, CDCl₃) δ -13.7 (10B), 5.5 (1B). Anal. Calcd. for C₂₅H₅₀B₁₁N₂O₃: C, 56.48; H, 9.48; N, 2.63. Found: C, 56.40; H, 9.55; N, 2.68.

5.2.8 Ester of [closo-1-CB₁₁H₁₀-1-COOH-12-(1-(4-C₇H₁₅O-C₅H₄N))] with 4-pentylphenol (**2[12]c**)

It was obtained using Method A in 74% yield after chromatography (CH₂Cl₂). The ester was purified by recrystallisation from toluene/*iso*-octane (3 \times) and then CH₃OH at -20°C (5 \times) to give a white crystalline solid: ¹H NMR (400 MHz, CDCl₃) δ 0.88 (t, *J* = 7.0 Hz, 3H), 0.90 (t, *J* = 6.8 Hz, 3H), 1.23–1.40 (m, 10H), 1.4–2.8 (br m, 10H), 1.41–1.50 (m, 2H), 1.58 (quint, *J* = 7.3 Hz, 2H), 1.86 (quint, *J* = 7.0 Hz, 2H), 2.56 (t, *J* = 7.7 Hz, 2H), 4.17 (t, *J* = 6.5 Hz, 2H), 6.94 (d, *J* = 8.5 Hz, 2H), 7.03 (d, *J* = 7.5 Hz, 2H),

7.12 (d, *J* = 8.5 Hz, 2H), 8.45 (d, *J* = 7.4 Hz, 2H); {¹H}¹¹B NMR (128 MHz, CDCl₃) δ -13.5 (10B), 5.9 (1B). Anal. Calcd. for C₂₅H₄₄B₁₁NO₃: C, 57.13; H, 8.44; N, 2.67. Found: C, 57.27; H, 8.36; N, 2.71.

5.2.9 Ester of [closo-1-CB₁₁H₁₀-1-COOH-12-(1-(4-C₇H₁₅O-C₅H₄N))] and 4-butoxyphenol (**2[12]d**)

It was obtained using Method A in 69% yield after chromatography (CH₂Cl₂). The ester was purified by recrystallisation from toluene/*iso*-octane (2 \times), EtOH at -20°C (2 \times) and then CH₃OH at -20°C (4 \times) to give a white crystalline solid: ¹H NMR (400 MHz, CDCl₃) δ 0.90 (t, *J* = 6.8 Hz, 3H), 0.96 (t, *J* = 7.4 Hz, 3H), 1.24–1.40 (m, 6H), 1.4–2.8 (br m, 10H), 1.41–1.52 (m, 4H), 1.74 (quint, *J* = 7.0 Hz, 2H), 1.86 (quint, *J* = 7.0 Hz, 2H), 3.92 (t, *J* = 6.5 Hz, 2H), 4.17 (t, *J* = 6.5 Hz, 2H), 6.82 (d, *J* = 9.1 Hz, 2H), 6.94 (d, *J* = 9.1 Hz, 2H), 7.03 (d, *J* = 7.5 Hz, 2H), 8.45 (d, *J* = 7.4 Hz, 2H); {¹H}¹¹B NMR (128 MHz, CDCl₃) δ -13.5 (10B), 5.9 (1B). Anal. Calcd. for C₂₄H₄₂B₁₁NO₄: C, 54.65; H, 8.03; N, 2.66. Found: C, 54.84; H, 8.20; N, 2.65.

5.2.10 Ester of [closo-1-CB₁₁H₁₀-1-COOH-12-(1-(4-C₇H₁₅O-C₅H₄N))] and 4-cyanophenol (**2[12]e**)

It was obtained using Method A in 69% yield after chromatography (CH₂Cl₂). The ester was purified by recrystallisation from EtOAc/hexane (2 \times), toluene/*iso*-octane (2 \times) and then CH₃OH at -20°C to give a white crystalline solid: ¹H NMR (400 MHz, CDCl₃) δ 0.90 (t, *J* = 6.8 Hz, 3H), 1.25–1.40 (m, 6H), 1.4–2.8 (br m, 10H), 1.41–1.51 (m, 2H), 1.86 (quint, *J* = 7.0 Hz, 2H), 4.18 (t, *J* = 6.5 Hz, 2H), 7.04 (d, *J* = 7.4 Hz, 2H), 7.20 (d, *J* = 8.8 Hz, 2H), 7.65 (d, *J* = 8.7 Hz, 2H), 8.44 (d, *J* = 7.4 Hz, 2H); {¹H}¹¹B NMR (128 MHz, CDCl₃) δ -13.3 (10B), 6.1 (1B). Anal. Calcd. for C₂₁H₃₃B₁₁N₂O₃: C, 52.50; H, 6.92; N, 5.83. Found: C, 52.76; H, 6.73; N, 5.75.

5.2.11 Ester of [closo-1-CB₁₁H₁₀-1-COOH-12-(1-(4-C₇H₁₅O-C₅H₄N))] and 2-(4-hexylphenyl)-5-hydroxypyrimidine (**2[12]f**)

It was obtained using Method A in 84% yield after chromatography (CH₂Cl₂). The ester was purified by recrystallisation from toluene/CH₃CN (4 \times) to give a white crystalline solid: ¹H NMR (400 MHz, CDCl₃) δ 0.88–0.91 (m, 6H), 1.22–1.40 (m, 12H), 1.41–1.50 (m, 2H), 1.65 (quint, *J* = 7.3 Hz, 2H), 1.4–2.8 (br m, 10H), 1.86 (quint, *J* = 6.9 Hz, 2H), 2.66 (t, *J* = 7.6 Hz, 2H), 4.18 (t, *J* = 6.5 Hz, 2H), 7.04 (d, *J* = 7.2 Hz, 2H), 7.27 (d, *J* = 8.3 Hz, 2H), 8.29 (d, *J* = 8.1 Hz, 2H), 8.44 (d, *J* = 7.1 Hz, 2H), 8.58 (s,

2H); $\{^1\text{H}\}^{11}\text{B}$ NMR (128 MHz, CDCl_3) δ -13.3 (10B), 6.1 (1B). Anal. Calcd. for $\text{C}_{30}\text{H}_{48}\text{B}_{11}\text{N}_3\text{O}_3$: C, 58.34; H, 7.83; N, 6.80. Found: C, 58.47; H, 7.62; N, 6.76.

5.2.12 Ester of [*closo-1-CB₉H₈-1-COOH-10-(1-(4-C₇H₁₅O-C₅H₄N))*] and 2-(hexylphenyl)-5-hydroxypyrimidine (2[10]f)

It was obtained using Method A in 77% yield after chromatography. The ester was purified by recrystallisation from *iso*-octane/toluene (2x) and then EtOAc/hexane (2x) to give a white crystalline solid: ^1H NMR (400 MHz, CDCl_3) δ 0.75–2.60 (br m, 8H), 0.89 (t, J = 6.6 Hz, 3H), 0.92 (t, J = 6.8 Hz, 3H), 1.23–1.47 (m, 12H), 1.53 (quint, J = 7.3 Hz, 2H), 1.67 (quint, J = 7.3 Hz, 2H), 1.95 (quint, J = 7.0 Hz, 2H), 2.69 (t, J = 7.7 Hz, 2H), 4.31 (t, J = 6.5 Hz, 2H), 7.31 (pseudo t, J = 7.3 Hz, 4H), 8.36 (d, J = 8.1 Hz, 2H), 8.88 (s, 2H), 9.09 (d, J = 7.0 Hz, 2H); $\{^1\text{H}\}^{11}\text{B}$ NMR (128 MHz, CDCl_3) δ -20.5 (4B), -15.4 (4B), 43.0 (1B). Anal. Calcd. for $\text{C}_{30}\text{H}_{46}\text{B}_9\text{N}_3\text{O}_3$: C, 60.66; H, 7.81; N, 7.07. Found: C, 60.88; H, 7.58; N, 7.04.

5.3 Preparation of 12-(4-heptyloxyphenyl)-*p*-carborane-1-carboxylic acid (3[12]) [13]

A solution of 1-(4-heptyloxyphenyl)-*p*-carborane [15] (8 [12], 1.39 g, 4.16 mmol) in anhydrous THF (20 mL) at 0°C was treated with *n*-BuLi (6.6 mL, 12.5 mmol, 1.9 M in hexanes). The reaction mixture was warmed to RT, and subsequently cooled back to 0°C, and dry CO_2 was bubbled through the solution for 30 min. The reaction mixture was evaporated to dryness and the residue washed with pentane. Et_2O (20 mL) and 10% HCl (20 mL) were added, and the Et_2O layer was separated. The aqueous layer was further extracted with Et_2O (3 × 20 mL). The organic layers were combined, washed with H_2O , dried (Na_2SO_4), and evaporated to dryness. The tacky white solid was washed with hot H_2O (2×) to remove residual valeric acid and dried *in vacuo*, providing 1.45 g (92% yield) of crude acid 3[12]. The acid was further purified by recrystallisation from aq. MeOH, CH_3CN , and *iso*-octane (2×): mp 175°C; ^1H NMR (400 MHz, CDCl_3) δ 0.88 (t, J = 6.8 Hz, 3H), 1.22–1.45 (m, 8H), 1.73 (quint, J = 7.0 Hz, 2H), 1.5–3.5 (br m, 10H), 3.87 (t, J = 6.6 Hz, 2H), 6.66 (d, J = 9.0 Hz, 2H), 7.05 (d, J = 9.0 Hz, 2H); $\{^1\text{H}\}^{11}\text{B}$ NMR (128 MHz, CDCl_3) δ -13.3 (5B), -12.3 (5B). Anal. Calcd. for $\text{C}_{16}\text{H}_{30}\text{B}_{10}\text{O}_3$: C, 50.77; H, 7.99. Found: C, 50.82; H, 7.92.

5.4 Preparation of [*closo-1-CB₁₁H₁₀-1-COOH-12-(4-C₇H₁₅OC₅H₄N)*] (4[12])

A slightly yellow solution of [*closo-1-CB₁₁H₁₀-1-COOH-10-NH₃*] (5[12], 1.02 g; 5.00 mmol) and 4-heptyloxyppyridine [26] (30 mL) was stirred at -20°C. $[\text{NO}]^+[\text{PF}_6]^-$ (5.42 g, 31 mmol) was added in six portions every 10–15 min and the solution was allowed to warm to RT and stirred for 8 h. As the reaction progressed, the solution became a yellow suspension and heat was produced. The suspension was saturated with hexanes (3 × 30 mL) to remove excess 4-heptyloxyppyridine and decanted. The yellow residue was treated with 10% HCl (30 mL) and the solution was extracted with Et_2O (3 × 20 mL). The Et_2O extracts were combined, dried (Na_2SO_4), and evaporated to give crude acid 4[12] as yellowish solid. The crude acid was passed through a short silica gel plug ($\text{CH}_3\text{OH}/\text{CH}_2\text{Cl}_2$, 1:9) giving 120 mg (6% yield) of pure acid as an off-white solid. An analytical sample of 4[12] was prepared by recrystallisation from toluene/ CH_3CN (3×): mp 189°C; ^1H NMR (400 MHz, CD_3CN) δ 0.90 (t, J = 6.9 Hz, 3H), 1.26–1.50 (m, 8H), 1.4–2.8 (br m, 10H), 1.81 (quint, J = 7.0 Hz, 2H), 4.23 (t, J = 6.6 Hz, 2H), 7.15 (d, J = 7.5 Hz, 2H), 8.40 (d, J = 7.4 Hz, 2H); $\{^1\text{H}\}^{11}\text{B}$ NMR (128 MHz, CD_3CN) δ -14.4 (5B), -13.6 (5B), 5.9 (1B). Anal. Calcd. for $\text{C}_{14}\text{H}_{30}\text{B}_{11}\text{NO}_3$: C, 44.33; H, 7.97; N, 3.69. Found: C, 44.31; H, 7.83; N, 3.49.

5.5 Preparation of [*closo-1-CB₁₁H₁₀-1-COOH-12-NH₃*] (5[12])

[*Closo-1-CB₁₁H₁₀-1-COOH-12-I*] $[\text{NEt}_4]^+$ (6[12], [10] 7.03 g, 15.8 mmol) was dissolved in a 1 M solution of LiHMDS in THF (300 mL, 0.24 mol) at RT under Ar. The mixture was stirred for 15 min before Pd_2dba_3 (0.97 g, 1.06 mmol) and 2-(dicyclohexylphosphino)biphenyl (0.70 g, 1.98 mmol) were added. The reaction turned brown and was stirred at reflux for 72 h. The reaction was cooled to 0°C and quenched with ice-cold 20% HCl (100 mL). THF was removed *in vacuo* and the aqueous layer was extracted with Et_2O (3 × 75 mL). The organic layers were dried (Na_2SO_4) and evaporated to dryness, giving the crude product in the form of brown oil.

The crude product was redissolved in Et_2O (30 mL), H_2O (75 mL) was added, and the Et_2O evaporated *in vacuo*. The aqueous layer was filtered, and the insoluble residue was redissolved in Et_2O . This process was repeated two times in order to ensure complete extraction of boron cluster-containing material to water. The aqueous layers were combined and treated with $[\text{NEt}_4]$

$^+[\text{Br}]^-$ (1.67 g, 7.95 mmol) to precipitate any deiodinated starting material, catalyst, and ligand by-products. The insoluble materials were filtered, the aqueous layer was acidified with conc. HCl (30 mL) and extracted with Et₂O (3 × 75 mL). The organic layer was dried (Na₂SO₄) and evaporated, leaving 1.29 g (40% yield) of amino acid **5**[**12**] as an off-white solid: $\{^1\text{H}\}^1\text{B}$ NMR (128 MHz, CD₃CN) δ -14.5 (5B), -13.8 (5B), 0.4 (1B). HRMS, calcd. for C₂H₁₄B₁₁NO₂ m/z 204.1976; found m/z 204.1969.

5.6 Preparation of 1-(4-heptyloxyphenyl)-*p*-carborane (**8**[**12**]) [**15**]

A suspension of 1-(4-hydroxyphenyl)-*p*-carborane [**14**] (**7**[**12**], 1.01 g, 4.26 mmol), heptyl tosylate [**27**] (4.15 g, 15.3 mmol), anhydrous K₂CO₃ (1.77 g, 12.8 mmol), and [NBu₄]⁺[Br]⁻ (0.14 g, 0.43 mmol) was stirred at reflux in anhydrous CH₃CN (50 mL) overnight. Precipitation was filtered off and washed with CH₂Cl₂. The filtrate was evaporated giving a colourless oil. The crude product was passed through a short silica gel plug (hexane), giving 1.26 g (89% yield) of product **7**[**12**] as a colourless oil: ^1H NMR (400 MHz, CDCl₃) δ 0.89 (t, J = 6.8 Hz, 3H), 1.22–1.46 (m, 8H), 1.73 (quint, J = 7.0 Hz, 2H), 1.5–3.5 (br m, 10H), 3.88 (t, J = 6.5 Hz, 2H), 6.67 (d, J = 9.0 Hz, 2H), 7.10 (d, J = 9.0 Hz, 2H); ^1B NMR (128 MHz, CDCl₃) δ -14.8 (5B), -12.0 (5B). Anal. Calcd. for C₁₅H₃₀B₁₀O: C, 53.86; H, 9.04. Found: C, 53.59; H, 9.30.

Funding

This work was supported by the NSF [grant number DMR-1207585].

References

- [1] Kirsch P, Bremer M. Nematic liquid crystals for active matrix displays: molecular design and synthesis. *Angew Chem Int Ed*. 2000;39:4216–4235. doi:10.1002/1521-3773(20001201)39:23<4216::AID-ANIE4216>>3.0.CO;2-K
- [2] Bremer M, Lietzau L. 1,1,6,7-tetrafluoroindanes: improved liquid crystals for LCD-TV application. *New J Chem*. 2005;29:72–74. doi:10.1039/b414312d
- [3] Blinov LM. Behavior of liquid crystals in electric and magnetic fields. In: Demus D, Goodby J, Gray GW, Spiess H-W, Vill V, editors. *Handbook of liquid crystals*. Vol. 1. New York (NY): Wiley-VCH; 1998. p. 477–534.
- [4] Blinov LM, Chigrinov VG. *Electrooptic effects in liquid crystal materials*. New York (NY): Springer-Verlag; 1994.
- [5] Kaszynski P, Pakhomov S, Gurskii ME, Erdyakov SY, Starikova ZA, Lyssenko KA, Antipin MY, Young VG Jr, Bubnov YN. 1-pyridine- and 1-quinclidine-1-boraadamantane as models for derivatives of 1-borabicyclo[2.2.2]octane. Experimental and theoretical evaluation of the B–N fragment as a polar isosteric substitution for the C–C group in liquid crystal compounds. *J Org Chem*. 2009;74:1709–1720. doi:10.1021/jo802504c
- [6] Ringstrand B, Kaszynski P. How much can an electric dipole stabilize a nematic phase? Polar and non-polar isosteric derivatives of [*closo*-1-CB₉H₁₀]⁻ and [*closo*-1,10-C₂B₈H₁₀]. *J Mater Chem*. 2010;20:9613–9615. doi:10.1039/c0jm02876b
- [7] Ringstrand B, Kaszynski P. High $\Delta\epsilon$ nematic liquid crystals: fluxional zwitterions of the [*closo*-1-CB₉H₁₀]⁻ cluster. *J Mater Chem*. 2011;21:90–95. doi:10.1039/c0jm02075c
- [8] Ringstrand B, Kaszynski P, Young VG Jr. Diazotization of the amino acid [*closo*-1-CB₉H₈-1-COOH-6-NH₃] and reactivity of the [*closo*-1-CB₉H₈-1-COO-6-N₂]⁻ anion. *Inorg Chem*. 2011;50:2654–2660. doi:10.1021/ic102557s
- [9] Pecyna J, Ringstrand B, Kaszynski P. Synthesis of 12-pyridinium derivatives of the [*closo*-1-CB₁₁H₁₂]⁻ cluster. (submitted).
- [10] Ringstrand B, Jankowiak A, Johnson LE, Kaszynski P, Pocięcha D, Górecka E. Anion-driven mesogenicity: a comparative study of ionic liquid crystals based on the [*closo*-1-CB₉H₁₀]⁻ and [*closo*-1-CB₁₁H₁₂]⁻ clusters. *J Mater Chem*. 2012;22:4874–4880. doi:10.1039/c2jm15448j
- [11] Ringstrand B, Kaszynski P, Young VG Jr, Janoušek JZ. Anionic amino acid [*closo*-1-CB₉H₈-1-COO-10-NH₃]⁻ and dinitrogen acid [*closo*-1-CB₉H₈-1-COOH-10-N₂]⁻ as key precursors to advanced materials: synthesis and reactivity. *Inorg Chem*. 2010;49:1166–1179. doi:10.1021/ic9021323
- [12] Pd-catalyzed amination of the parent [*closo*-1-CB₁₁H₁₁-12-I]⁻ under similar conditions in a microwave oven was recently reported: Konieczka SZ, Himmelspach A, Hailmann M, Finze M. Synthesis, characterization, and selected properties of 7- and 12-ammoniocarba-*closo*-dodecaboranes. *Eur J Inorg Chem*. 2013;134–146. doi:10.1002/ejic.201200969
- [13] Ohta K, Januszko A, Kaszynski P, Nagamine T, Sasnowski G, Endo Y. Structural effects in three-ring mesogenic derivatives of *p*-carborane and their hydrocarbon analogues. *Liq Cryst*. 2004;31:671–682. doi:10.1080/02678290410001670584
- [14] Endo Y, Iijima T, Yamakoshi Y, Fukasawa H, Miyaura C, Inada M, Kubo A, Itai A. Potent estrogen agonists based on carborane as a hydrophobic skeletal structure: a new medicinal application of boron clusters. *Chem Biol*. 2001;8:341–355. doi:10.1016/S1074-5521(01)00016-3
- [15] Douglass AG, Pakhomov S, Reeves B, Janoušek Z, Kaszynski P. Triphenylsilyl as a protecting group in the synthesis of 1,12-heterodisubstituted *p*-carboranes. *J Org Chem*. 2000;65:1434–1441. doi:10.1021/jo991588z
- [16] Zhao Y, Truhlar DG. The M06 suite of density functionals for main group thermochemistry, thermochemical kinetics, noncovalent interactions, excited states, and transition elements: two new functionals and systematic testing of four M06-class functionals and 12 other functionals. *Theor Chem Acc*. 2008;120:215–241.
- [17] Chan T-N, Lu Z, Yam W-S, Yeap G-Y, Imrie CT. Non-symmetric liquid crystal dimers containing an isoflavone moiety. *Liq Cryst*. 2012;39:393–402. doi:10.1080/02678292.2012.658712

- [18] Kaszynski P, Januszko A, Ohta K, Nagamine T, Potaczek P, Young VG Jr, Endo Y. Conformational effects on mesophase stability: numerical comparison of carborane diester homologous series with their bicyclo[2.2.2]octane, cyclohexane and benzene analogues. *Liq Cryst.* 2008;35:1169–1190. doi:10.1080/02678290802409775
- [19] Kaszynski P. *Closo*-boranes as structural elements for liquid crystals. In: Hosmane N, editor. *Boron science: new technologies & applications*. New York (NY): CRC Press; 2012. p. 305–338.
- [20] Gavrilovic DM. United States patent US 3.925.238. 1975; Liqcryst 5.0 database, compound #25521.
- [21] Januszko A, Glab KL, Kaszynski P, Patel K, Lewis RA, Mehl GH, Wand MD. The effect of carborane, bicyclo [2.2.2]octane and benzene on mesogenic and dielectric properties of laterally fluorinated three-ring mesogens. *J Mater Chem.* 2006;16:3183–3192. doi:10.1039/b600068a
- [22] Frisch MJ, Trucks GW, Schlegel HB, Scuseria GE, Robb MA, Scuseria GE, Robb MA, Cheeseman JR, Scalmani G, Barone V, Mennucci B, Petersson GA, Nakatsuji H, Caricato M, Li X, Hratchian HP, Izmaylov AF, Bloino J, Zheng G, Sonnenberg JL, Hada M, Ehara M, Toyota K, Fukuda R, Hasegawa J, Ishida M, Nakajima T, Honda Y, Kitao O, Nakai H, Vreven T, Montgomery Jr JA, Peralta JE, Ogliaro F, Bearpark M, Heyd JJ, Brothers E, Kudin KN, Staroverov VN, Kobayashi R, Normand J, Raghavachari K, Rendell A, Burant JC, Iyengar SS, Tomasi J, Cossi M, Rega N, Millam JM, Klene M, Knox JE, Cross JB, Bakken V, Adamo C, Jaramillo J, Gomperts R, Stratmann RE, Yazyev O, Austin AJ, Cammi R, Pomelli C, Ochterski JW, Martin RL, Morokuma K, Zakrzewski VG, Voth GA, Salvador P, Dannenberg JJ, Dapprich S, Daniels AD, Farkas O, Foresman JB, Ortiz JV, Cioslowski J, Fox DJ. *Gaussian 09*, revision A.02. Wallingford (CT): Gaussian; 2009.
- [23] Simon S, Duran M, Dannenberg JJ. How does basis set superposition error change the potential surfaces for hydrogen-bonded dimers? *J Chem Phys.* 1996;105:11024–11031. doi:10.1063/1.472902
- [24] Cossi M, Scalmani G, Rega N, Barone V. New developments in the polarizable continuum model for quantum mechanical and classical calculations on molecules in solution. *J Chem Phys.* 2002;117:43–54 and references therein. doi:10.1063/1.1480445
- [25] Pecyna J, Kaszyński P, Ringstrand B, Bremer M. Investigation of high $\Delta\epsilon$ derivatives of the [*closo*-1-CB₉H₁₀][−] anion for liquid crystal display applications. *J Mater Chem C.* 2014;2:2956–2964. doi:10.1039/c4tc00230j
- [26] Kaszynski P, Huang J, Jenkins GS, Bairamov KA, Lipiak D. Boron clusters in liquid crystals. *Mol Cryst Liq Cryst.* 1995;260:315–332. doi:10.1080/10587259508038705
- [27] Burns DH, Miller JD, Chan H-K, Delaney MO. Scope and utility of a new soluble copper catalyst [CuBr–LiSPh–LiBr–THF]: a comparison with other copper catalysts in their ability to couple one equivalent of a grignard reagent with an alkyl sulfonate. *J Am Chem Soc.* 1997;119:2125–2133. doi:10.1021/ja963944q